Vol 18 No 4, April 2009
1674-1056/2009/18(04)/1669-05

Chinese Physics B

© 2009 Chin. Phys. Soc.
and IOP Publishing Ltd

Spontaneous formation of single crystal ZnO nanohelices*

Wu Xiang(武 祥)[a)†], Cai Wei(蔡 伟)[b)], and Qu Feng-Yu(曲凤玉)[a)]

[a)] *College of Chemistry and Chemical Engineering, Harbin Normal University, Harbin 150025, China*

[b)] *School of Materials Science and Engineering, Harbin Institute of Technology, Harbin 150001, China*

(Received 13 August 2008; revised manuscript received 12 September 2008)

This paper reports a novel helix-like ZnO nanostructure with several tens of nanometres in thickness synthesized on a gold-coated Si substrate by thermal evaporation of zinc sulfide powder at 1020 °C. Transmission electron microscope characterization shows that as-synthesized ZnO nanohelices extend along $[01\bar{1}1]$ direction and the axial direction of the helix is along [0001] direction. A catalyst-intervened dislocation-induced growth mechanism has been suggested to explain the formation of the helix-like ZnO nanostructures. This study opens a new route to construct helix-like ZnO nanostructures by different evaporation sources.

Keywords: nanohelix, thermal evaporation, ZnO, growth mechanism
PACC: 8110B, 6146, 6870

1. Introduction

One-dimensional (1D) or quasi-1D nanomaterials with helix structures have stimulated worldwide interests of study due to special morphologies and novel physical properties. These 1D helical nanostructures can be expected to use as high sensitive mechanical resonators and advanced optical and electrical nanodevices.[1−5] Helix structures widely exist in biological and self-assembled organic systems. Deoxynbonucleic acid (DNA) molecules with double helix structure are the most representative example. The helical structure in bio-molecules exhibits special functions and plays a very important role in replication of new cells. It is well known that the driving forces for formation of the double helix structure of DNA are Van der Waals and hydrogen bond interactions.[6−8] Compared with biological systems, formation mechanisms for inorganic materials with helix structures are a little complicated. For example, Amelinckx *et al* [9] reported carbon nanotube (CNT) coils. The formation of the curved CNT is believed to originate from periodic arrangements of the paired carbon pentagon and heptagon rings. Zhang and co-workers[10] prepared helical crystalline SiC/SiO_2 core-shell nanowires by a chemical vapour deposition method, a screw-dislocation-induced growth mechanism was suggested to explain the formation of the helical complex nanostructures. Recently, Wang *et al* [11] discovered the ZnO nanosprings formed by rolling up single-crystal ZnO nanobelts. The balance of electrostatic interaction and the elastic deformation is a main reason for final helical morphology of obtained ZnO nanostructures. Furthermore, Motojiam[12] and Zhang[13] also observed amorphous micro- and nano-scaled C and Si_3N_4 whisker springs. The occurrence of the amorphous material springs is understood in terms of contact angle anisotropy model involved catalyst particles. These studies show that structure, component and synthesis route of inorganic materials determine the diversity of formation mechanism of obtained helix structures.

Herein, we report a kind of novel helix-like ZnO nanostructure prepared on the Au-coated Si substrate by thermal evaporation of ZnS powder at 1020 °C. Some stacking faults have been found to exist at the bent positions of the ZnO nanospring. It shows that occurrence of the stacking fault is the possible root for formation of the helix-like ZnO nanostructures. The role of Au catalyst in the formation of the stacking faults is discussed.

*Project supported by National Key Basic Research Project (Grant No 2003CB716900), Doctor Start-up Fund of Harbin Normal University (Grant No KGB200802), Natural Science Foundation of Heilongjiang Province (Grant No B2007-2), and the Science Technology and Research Project of Education Bureau, Heilongjiang Province (Grant No 11531229).

†Corresponding author. E-mail: wuxiang05@gmail.com

2. Experimental details

Synthesis of the ZnO nanohelices was carried out in a conventional horizontal tube furnace. Firstly, Au-coated silicon wafer was ultrasonically cleaned in acetone solution for 5 minutes and rinsed with deionized water, then dried in air. One gram commercial ZnS powder was put into an aluminium boat, then the boat and silicon wafer were positioned in a small quartz tube. Subsequently, the small quartz tube was placed in the centre of the large quartz tube inserted in the furnace. After the system was sealed, the furnace was pumped to eliminate air for 2 hours. After that, argon carrier gas with 5% hydrogen gas was flowed in through the system at a rate of 100 sccm. The furnace was heated to 1020 °C at the rate of 20 °C per minute and kept for 2 hours at the temperature. The chamber pressure was kept at 300 Torr (1 Torr=133 Pa). After the furnace was cooled to room temperature, the Si substrate was taken out and characterized by a field emission scanning electron microscope (SEM, Hitachi-4800) attached with an energy dispersive x-ray spectrum (EDX) instrument and a transmission electron microscope (TEM, JEOL 4000EX).

3. Results and discussion

As-grown product at collection temperature of about 600 °C was firstly characterized by SEM. Figure 1 shows a series of SEM images of the products from lower to higher resolution. In Fig.1(a), the low resolution SEM image shows that a large number of wire-like products were deposited on the Au-coated Si substrate. Further observation to the SEM images shows that the products are composed of nanowires, nanobelts and helical nanostructures. The nanowires have an average diameter of several tens of nanometres and an average length of several tens of micrometres. The nanobelts have an average width of 200 nm and an average length of several tens of micrometres. They take about 90% of the total products deposited on the Si substrate while yield of the helical nanostructures only takes about 10%. The EDX measurement indicates that the products only consist of Zn and O elements. The ratio of Zn/O is closed to 1:1. This implies that these products collected on the Si substrate are ZnO (showed in Fig.2). A series of highly magnified SEM image of a helix-like ZnO nanobelt are shown from Fig.1(b) to Fig.1(d). Width of the helical ZnO nanobelt is about 200 nm and thickness is about several tens of nanometres. It has a uniform turn-to-turn spacing (TTS) of about 150 nm and an average diameter of 300 nm. The longest ZnO helix can achieve several tens of micrometres.

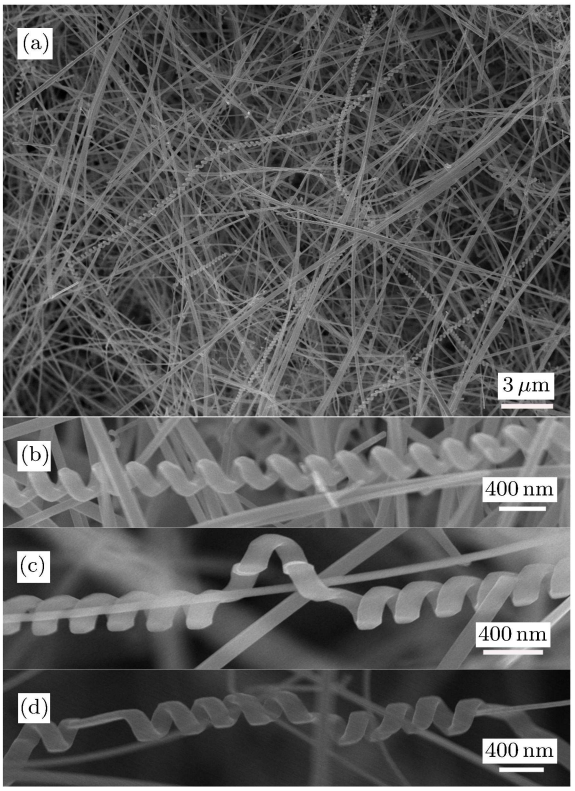


Fig.1. SEM images of as-synthesized ZnO products. (a) A low magnified SEM image of as-grown wire-like product, (b–d) High-magnification SEM images of the ZnO nanohelices.

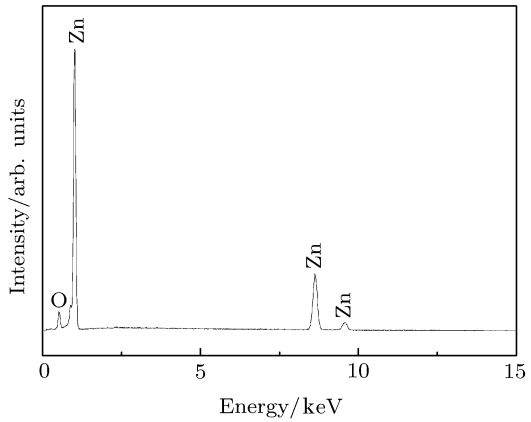


Fig.2. An EDX spectrum of as-synthesized ZnO nanohelices.

To further gain an insight into structure and possible growth process of the ZnO helices, we analysed the as-synthesized ZnO helices by a TEM. Figures 3(a) and 3(b) are typical bright field and dark field

TEM images of the ZnO helix segment, respectively. The inset is a selected area electron diffraction pattern at its top region. The TEM characterization results clearly show that the helix has a hexagonal single crystal structure. The ZnO nanobelt with rectangle section extendedly grows along $[01\bar{1}1]$ direction. Axial direction of the ZnO helix is [0001] direction. As the incident electron beam is parallel to $[2\bar{1}\bar{1}0]$ zone axis, the top and bottom planes of the ZnO nanobelt are $(\pm 2\ \bar{1}\bar{1}0)$ and two side surfaces are $(\pm 01\bar{1}\bar{2})$. Figure 3(c) is a local bright field TEM image and Fig.3(d) is corresponding high resolution TEM image of the top nanobelt region of the ZnO nanohelix. Observed distance between two adjacent parallel lattice planes is about 0.26 nm, being consistent with that of (0002) plane. Figure 3(e) is a dark field TEM image at bent region of the as-grown ZnO helix. Stacking faults in c-plane can be clearly seen.

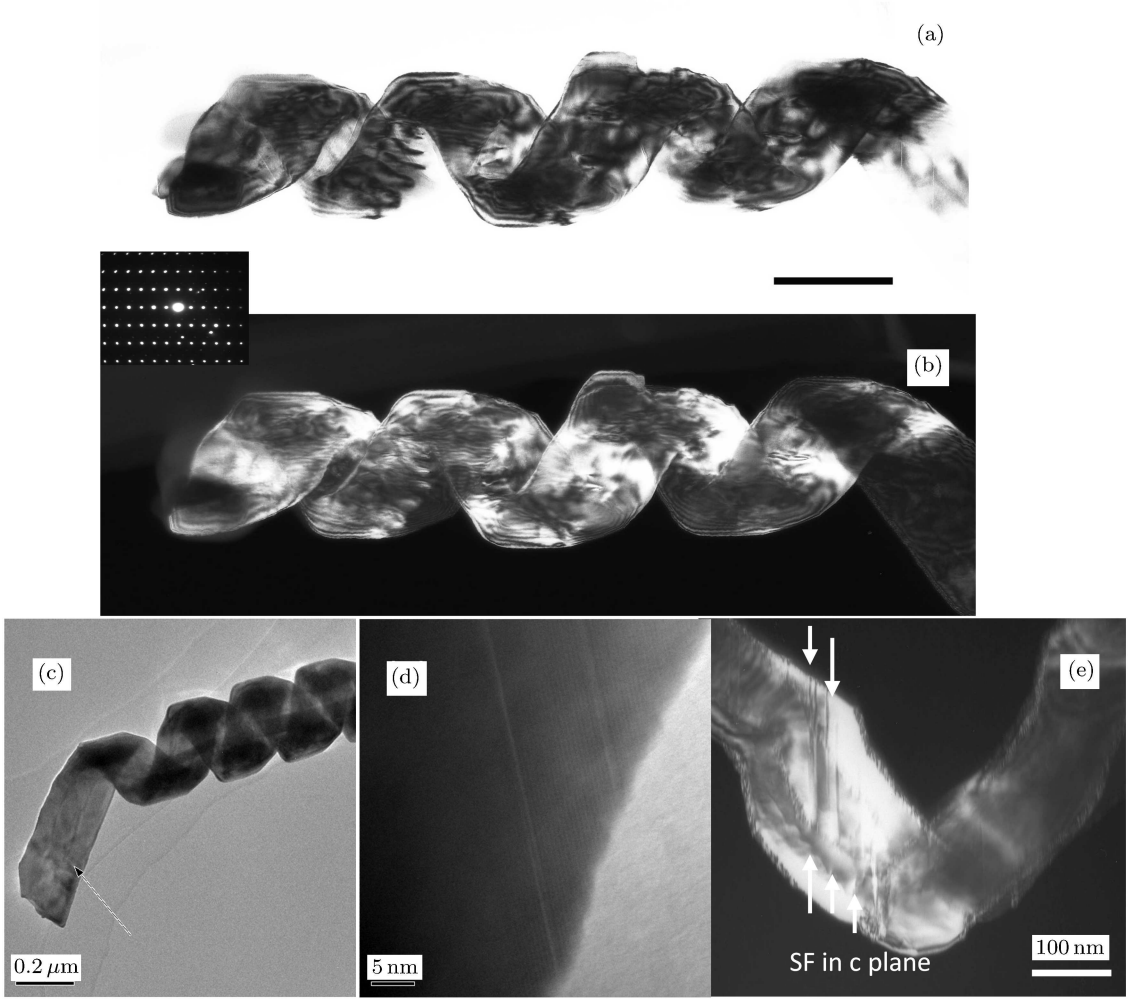


Fig.3. Typical TEM images of the ZnO nanohelices. (a) A bright field TEM image of the ZnO helix segment; (b) A corresponding dark field TEM image of the same ZnO helix segment, the insert in Figs.3(a) and 3(b) is an ED pattern of top belt region of the ZnO helix segment, clearly showing the growth direction $(01\bar{1}1)$ and axial direction (0001) of the helical ZnO nanobelt; (c) a high-magnification TEM image of ZnO nanohelix segment and (d) A corresponding high-resolution TEM image of a small ZnO belt side region, showing lattice inter-plane distance of (0002) planes. The width of belt is about 200 nm, (e) a dark field TEM image of the ZnO nanohelix at a turn region, demonstrating clear stacking faults in c-planes.

In general, formation of straight ZnO nanowires and nanobelts can be described in terms of vapour–liquid–solid (VLS) or vapour–solid growth mechanism depending on existence of catalyst or not. Wagner and Ellis firstly proposed the VLS mechanism.[14] In the VLS model, a catalyst liquid droplet was believed to

play a critical role for the formation of the nanowires and nanobelts. Under certain conditions of temperature and vapour pressure, the vapour phase material from surrounding can be dissolved in the liquid droplet in the form of either an element or a molecular precursor. As the material concentration achieves supersaturation in the catalyst, the material will overflow and grow into the nanowires or nanobelts. The nanowires or nanobelts can continuously extend as long as a sufficient quantity of vapour reactant is provided. It is clear from the VLS mechanism that the catalyst status determines the formation of the straight nanowires or nanobelts. In our present case, Au coated on the Si substrate can serve as a catalyst, but no Au particles have been found on tops or bottoms of the obtained wire- and belt-like products by SEM and TEM observations. An explanation is that the Au particle catalysts have probably been evaporated when the growth of the ZnO nanowires and nanobelts finishes.[15] Therefore, we suggest that the formation of the ZnO nanowires and nanobelts probably originates from the catalysis of the Au nanoparticles and obeys the VLS mechanism.

It is surprised that helix-like ZnO nanowires and nanobelts occur together with those straight types. Theoretical calculation[16] shows that straight strings can transfer into spontaneous helical chirality because of entropic interactions. The optimal configuration is energetically preferred. Two possible formation processes can be assumed when considering nanohelix evolution and growth. The first is that regular nanowire and nanobelt firstly grow, and subsequently follow by a helical rotation of the formed nanostructures. The second is nucleation and growth of a helical structure. For the case of the nanohelix structures induced by catalysts, the second process is more favoured in terms of the VLS mechanism. In our case, at high temperature, ZnS powder first evaporates into ZnS vapour, which then reacts with H_2 gas to form Zn vapour and H_2S gas. H_2S gas can be taken away by Ar/H_2 carrier gas. The Zn vapour can be dissolved in Au nanoparticle catalyst to form Zn–Au alloy. When solubility of the Zn vapour in the Au nanoparticle reaches supersaturation, the Zn can overflow from the Au nanoparticle catalyst and react with residual oxygen in the closed system to form ZnO nuclei at the catalyst interface. With the reaction progress, ZnO nuclei can form ZnO nanowire or nanobelt. As mentioned before, driving forces for the formation of helical structures in biological systems are Van der Waals and H-bonding interactions. What is the driving force for the formation of the helical ZnO nanobelts? Based on our TEM observation, we have found some stacking faults existing in c-plane of obtained single crystal ZnO helices. Therefore, we think that the formation of the ZnO helices is due to the stacking faults in the ZnO nanobelts initially introduced at the catalyst/ZnO interface. The stacking faults are probably caused by local perturbations due to motion of the Au catalytic particle. As a result, a nonzero torque can be created at the catalyst/ZnO interface, which leads to an asymmetric growth front. Further reaction and self-catalyst assisted growth induces the production of the ZnO nanohelices.

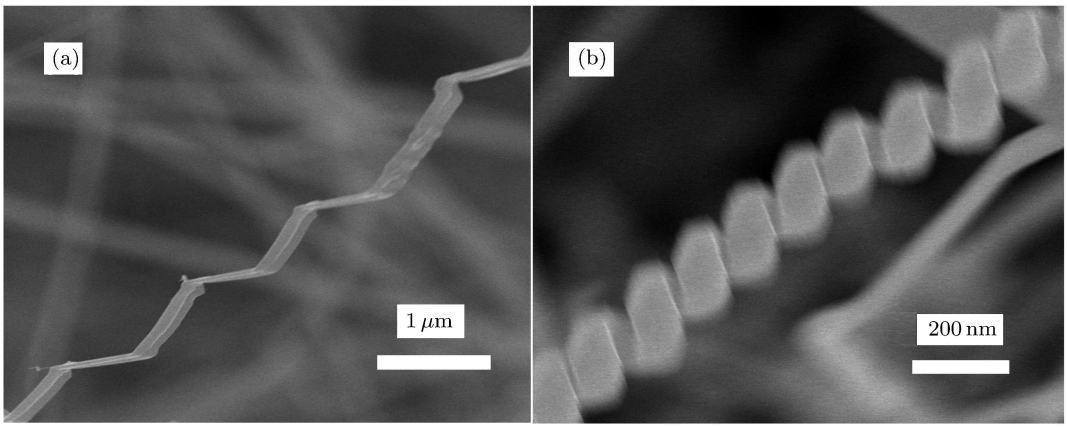


Fig.4. SEM images of the ZnO nanohelices grown (a) in higher temperature zone of about 800 °C, (b) in higher temperature zone of about 500 °C.

Another argument supporting the catalyst-induced mechanism is the appearance of the ZnO helices with fluctuated TTS and straight-helical complex nanostructures. The fact implies that the morphologies of obtained ZnO helices are close related to fluctuation of growing front of the ZnO nanohelix. In addition, the helical ZnO nanobelts collected at different temperature regions exhibit various TTS. Figure 4 provides SEM images of the ZnO nanohelices collected at the regions of about 800 °C and 500 °C. At higher temperature of about 800 °C, the ZnO helices with a larger TTS of about 1.5 μm occur. At lower temperature zone of about 500 °C, the ZnO helices have a smaller TTS of about 100 nm. This phenomenon can be reasonably explained in terms of the difference of relative movement rates of catalyst particles at different temperatures. Because catalyst particles run faster at high temperature than at low temperature, the ZnO nanohelices grown at higher temperature possess larger TTS than those obtained at lower temperature. Furthermore, to further prove the role of the Au catalyst, ZnO product was also prepared in the case without the Au catalyst on Si substrate under the same other conditions. Only were ZnO nanobelts with a high yield deposited on the Si substrate (see Fig.5). This illustrates that the Au catalyst is indeed responsible for the formation of the ZnO helices. In fact, growth dynamics process of helical nanowires and nanobelts is considerable complicated, the effect of some other factors, such as un-reacted ZnS and impurities, on the formation of the helical ZnO nanobelts are still not clear. For example, mismatch induced strain between ZnS and ZnO also can induce bending of the nanobelts.[17] To completely gain an insight into the formation root of the ZnO helix, more investigations are needed.

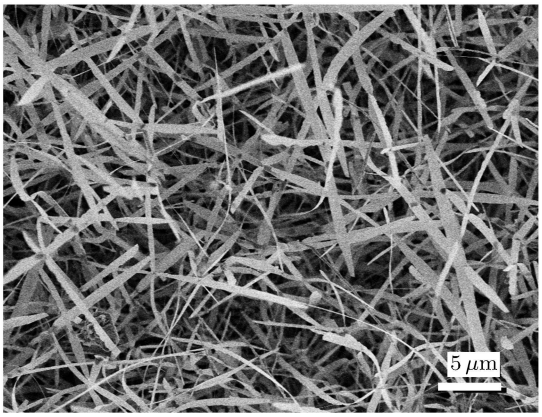


Fig.5. A typical of SEM image of as-synthesized ZnO product without gold as a catalyst. Only straight ZnO nanobelts can be formed.

4. Conclusion

In summary, we have successfully synthesized ZnO nanohelices by thermally evaporating ZnS powder at 1020 °C in a horizontal tube furnace. The Au catalyst is believed to play an important role for the formation and further evolution of the ZnO helices. The formation of ZnO stacking faults at the interface of catalyst/ZnO is the possible origination for the nucleation and subsequent growth of the helical ZnO nanostructure. The ZnO nanohelices are expected to have potential applications in biosensors, resonators, micromechanical and nanopiezotronics devices.

References

[1] Singh J, Liu D, Ye D, Picu R, Lu T and Wang G 2004 *Appl. Phys. Lett.* **84** 3657
[2] Kesapragada S, Victor P, Nalamasu O and Gall D 2006 *Nano Lett.* **6** 854
[3] Bell D, Bauert T, Zhang L, Dong L, Sun Y, Grützmacher D and Nelson B 2007 *Nanotechnology* **18** 055304
[4] Liu R B, Pan A L, Wang F F and Zou B S 2007 *Chin. Phys.* **16** 1129
[5] Fonseca A and Galvao D 2004 *Phys. Rev. Lett.* **92** 175502
[6] Rhodes D and Klug A 1980 *Nature* **286** 573
[7] Weber P and Salemm F 1980 *Nature* **287** 82
[8] Hirschberg J, Brunsveld L, Ramzi A, Vekemans J, Sijbesma R and Meijer E 2000 *Nature* **407** 167
[9] Amelinckx S, Zhang X, Bernaerts D, Zhang X and Nagy V 1994 *Science* **265** 635
[10] Zhang H, Wang C, Buck E and Wang L 2003 *Nano Lett.* **3** 577
[11] Yang R S, Ding Y and Wang Z L 2004 *Nano Lett.* **4** 1309
[12] Motojima S, Ueno S, Hattori T and Goto K 1989 *Appl. Phys. Lett.* **54** 1001
[13] Zhang D, Alkhateeb A, Han H, Mahmood H, McIlroy D and Norton M 2003 *Nano Lett.* **3** 983
[14] Wagner R and Ellis W 1964 *Appl. Phys. Lett.* **4** 89
[15] Bae S, Lee J, Jung H, Park J and Ahn J 2005 *J. Am. Chem. Soc.* **127** 10802
[16] Gulseren O, Ercolessi F and Tosatti E 1998 *Phys. Rev. Lett.* **80** 3775
[17] Wu X, Jiang P, Ding Y, Cai W, Xie S S and Wang Z L 2007 *Adv. Mater.* **19** 2319